

Operation bandwidth of forward stimulated Brillouin scattering in silicon Brillouin active membrane waveguides

Heedeuk Shin¹, Jonathan A. Cox², Robert Jarecki², Andrew Starbuck², Wenjun Qiu³, Zheng Wang⁴, and Peter T. Rakich¹

¹ Department of Applied Physics, Yale University, New Haven, Connecticut 06520, USA.

² Sandia National Laboratories, PO Box 5800, Albuquerque, NM 87185, USA

³ Department of Physics, Massachusetts Institute of Technology, Cambridge, Massachusetts 02139, USA

⁴ Department of Electrical and Computer Engineering, University of Texas at Austin, Austin, TX 78758, USA

Author e-mail address: peter.rakich@yale.edu

Abstract: We studied the operation bandwidth of forward stimulated Brillouin scattering with the optical waveguide width in silicon Brillouin active membrane waveguides. Waveguides with narrow width yield Brillouin resonant features over wide frequency range, but waveguides with broad width induce less nonlinear absorption.

OCIS codes: (1902640) Stimulated scattering, modulation, etc; (1905970) Semiconductor nonlinear optics including MQW; (1904390) Nonlinear optics, integrated optics

Stimulated Brillouin scattering (SBS) is the nonlinear optical phenomena of light scattering by acoustic waves through media. Since its first observation in 1964 [1], SBS has been intensively studied in optical fibers as the basis for various applications. Optical forces by electrostriction and radiation pressure are dramatically enhanced at nanoscales [2,3,4], with strong confinement of both the photonic and phononic modes through a waveguide, on-chip Brillouin active technologies in silicon nano-photonics can open up a host of wide-band signal processing capabilities.

Recently, we reported the first ever experimental demonstration of forward SBS in silicon waveguide as in Fig. 1a [5]. The Brillouin active membrane (BAM) waveguide consist of silicon waveguide core guiding optical waves and two side silicon nitride membrane wings guiding phononic waves as shown in Fig. 1b-c. The thickness of silicon nitride membrane, t , is about 124 nm and the waveguide height, c , is about 194 nm. Fig. 1d shows the geometric scheme of near the silicon waveguide core and Fig. 1e exhibits the guided optical field distribution in the waveguide core. This optical mode yields the optical forces by electrostriction force and radiation pressure which are displayed in Fig. 1f and g, respectively. The combination of these optical forces yields phonon vibration guided between two air slot boundaries. When the guided phonon modes satisfy the phase matching condition as in Fig. 1i, it yields strong resonant Brillouin active features as shown in Fig. 1h.

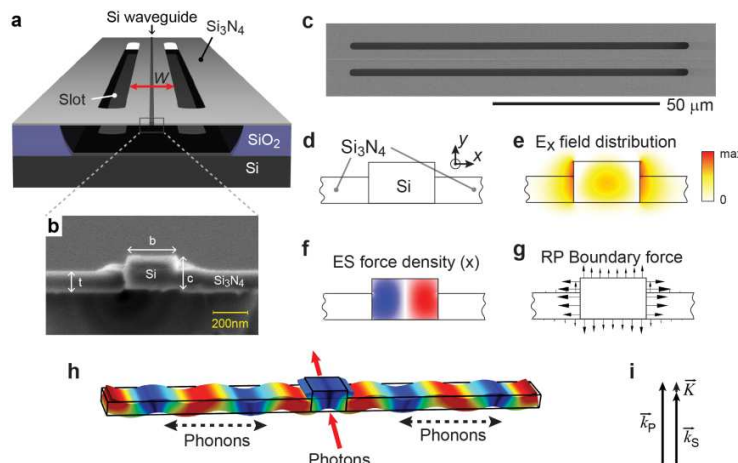


Figure 1 Hybrid photonic-phononic waveguide enabling independent control of the optical and phonon modes. (a) Diagram showing anatomy of the Brillouin-active membrane (BAM) waveguide. (b) High-resolution SEM cross-section of the silicon waveguide core with width $b=313$ nm and height $c=194$ nm within the silicon nitride membrane with thickness $t=124$ nm. (c) Top-down SEM image of a unit of the BAM waveguide. (d,e) The waveguide cross-section and the computed E_x field profile of the optical mode. (f,g) The computed x component of the electrostriction (ES) force densities and radiation pressure (RP)-induced boundary forces generated within silicon, respectively. (h) A simulated guided phonon mode in a section of the BAM waveguide. (i) Phase matching condition of forward stimulated Brillouin scattering. The sum of scattered photon wavevector, \vec{k}_s , and guided phonon wavevector, \vec{K} , equal to that of pump photon, \vec{k}_p .

The Brillouin active nonlinearities for a waveguide width of 313 nm have been observed over wide range of frequency (1-20 GHz) in ref. [5]. The tight confinement of optical mode in silicon waveguide enables this wide operation bandwidth, but it also induces large nonlinear absorption caused by two-photon absorption and two-photon-absorption induced free carrier absorption [6], yielding shorter effective propagation length of waveguide and lower power handling. To study the operation bandwidth with waveguide width, we fabricate two different BAM waveguides for $b = 950$ nm and $b = 313$ nm widths with same phononic dimension, $W = 3.8$ μm . The computed x component of electric field and the corresponding ES force density distribution for the 950-nm waveguide are shown in Fig. 2a and b and compared with these in Fig. 1e and f, respectively. The experimental measurements of the normalized RF power from two BAM waveguides are performed with the heterodyne measurement in ref. [5]. As shown in Fig. 2c, both waveguides has similar Brillouin active nonlinearities except that the 950-nm waveguide can induce Brillouin active resonant features at only over 1-11 GHz, showing that the narrower optical waveguide width can yield Brillouin resonant features over wider frequency range. However, due to the less tight optical confinement, the overall absorption in wider waveguide is less than that in narrower waveguide.

The independent control of photonic and phononic modes in BAM waveguides enables the study of the optimum waveguide width for desired operation bandwidth and less absorption coefficient. This study reveals that waveguides with narrow width yield Brillouin resonant features over wide frequency range, but waveguides with broad width induce less nonlinear absorption. This study could be essential for the BAM waveguides to provide a host of new coherent signal-processing technologies.

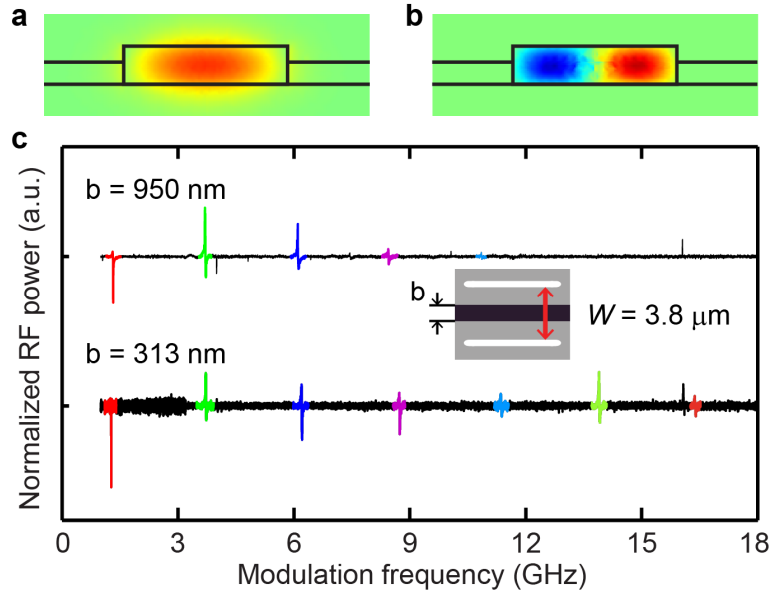


Figure 2 Normalized RF power for different waveguide widths with same phononic dimension. (a) The waveguide cross-section and the computed Ex field profile of the optical mode. (b) The computed x component of the ES force density distribution. (c) The normalized RF power for different waveguide width $b=950$ nm (upper) and $b=313$ nm (lower), respectively. Both have same phononic dimension, $W=3.8 \mu\text{m}$.

Acknowledgements

Sandia Laboratory is operated by Sandia Co., a Lockheed Martin Company, for the U.S. Department of Energy's NNSA under Contract No. DE-AC04- 94AL85000. This work was supported by the DDRE under Air Force Contract No. FA8721-05-C-000, the MesoDynamic Architectures program at DARPA under the direction of Dr. Jeffrey L. Rogers, and Sandia's Laboratory Directed Research and Development program under Dr. Wahid Hermina.

References

- [1] R. Chiao, *et al.*, Phys. Rev. Lett. **12**, 592 (1964).
- [2] P. T. Rakich, *et al.*, Opt. Express **18**, 14439 (2010).
- [3] P. T. Rakich, *et al.*, Phys. Rev. X **2**, 011008 (2012).
- [4] W. Qiu, *et al.*, Opt. Express **21**, 31402 (2013).
- [5] H. Shin, *et al.*, Nat. Comm. **4**, 1944 (2013).
- [6] Q. Lin, *et al.*, Opt. Express **15**, 16604 (2007).